condensed matter

MDPI

Article

The Potential of EuPRAXIA@SPARC_LAB for Radiation Based Techniques

Antonella Balerna [1], Samanta Bartocci [2], Giovanni Batignani [3], Alessandro Cianchi [4,5], Enrica Chiadroni [1], Marcello Coreno [1,6], Antonio Cricenti [6], Sultan Dabagov [1,7,8], Andrea Di Cicco [9], Massimo Faiferri [2], Carino Ferrante [3,10], Massimo Ferrario [1], Giuseppe Fumero [3,11], Luca Giannessi [12,13], Roberto Gunnella [9], Juan José Leani [14], Stefano Lupi [3,15], Salvatore Macis [4,5], Rosa Manca [2], Augusto Marcelli [1,6], Claudio Masciovecchio [12], Marco Minicucci [9], Silvia Morante [4,5], Enrico Perfetto [4,16], Massimo Petrarca [3,15], Fabrizio Pusceddu [2], Javad Rezvani [1], José Ignacio Robledo [14], Giancarlo Rossi [4,5,17], Héctor Jorge Sánchez [14,18], Tullio Scopigno [3,10], Gianluca Stefanucci [4,5], Francesco Stellato [4,5,*], Angela Trapananti [9] and Fabio Villa [1]

1 Istituto Nazionale di Fisica Nucleare INFN—Laboratori Nazionali di Frascati, via E. Fermi 40, 00044 Frascati, Italy; Antonella.Balerna@lnf.infn.it (A.B.); Enrica.Chiadroni@lnf.infn.it (E.C.); marcello.coreno@elettra.eu (M.C.); sultan.dabagov@lnf.infn.it (S.D.); Massimo.Ferrario@lnf.infn.it (M.F.); augusto.marcelli@lnf.infn.it (A.M.); Javad.Rezvani@lnf.infn.it (J.R.); fabio.Villa@lnf.infn.it (F.V.)

2 Dipartimento di Architettura, Design e Urbanistica, Università degli studi di Sassari, Palazzo del Pou Salit—Piazza Duomo, 6-07041 Alghero, Italy; samantabartocci@gmail.com (S.B.); faiferri@uniss.it (M.F.); mancarosa@yahoo.it (R.M.); fabrizio_pusceddu@yahoo.it (F.P.)

3 Dipartimento di Fisica, Università degli studi di Roma "La Sapienza", P.le Aldo Moro 2, 00185 Rome, Italy; giovanni.batignani@roma1.infn.it (G.B.); carino.ferrante@iit.it (C.F.); giuseppe.fumero@gmail.com (G.F.); stefano.lupi@roma1.infn.it (S.L.); massimo.petrarca@roma1.infn.it (M.P.); tullio.scopigno@uniroma1.it (T.S.)

4 Dipartimento di Fisica, Università degli Studi di Roma Tor Vergata, Via della Ricerca Scientifica 1, 00133 Rome, Italy; Alessandro.Cianchi@roma2.infn.it (A.C.); Salvatore.Macis@roma2.infn.it (S.M.); silvia.morante@roma2.infn.it (S.M.); Enrico.Perfetto@roma2.infn.it (E.P.); Giancarlo.Rossi@roma2.infn.it (G.R.); stefanucci@roma2.infn.it (G.S.)

5 Istituto Nazionale di Fisica Nucleare (INFN) Sezione di Roma Tor Vergata, Via della Ricerca Scientifica 1, 00133 Rome, Italy

6 Istituto di Struttura della Materia (ISM)-Consiglio Nazionale delle Ricerche (CNR), via Fosso del Cavaliere 100, 00133 Rome, Italy; antonio.cricenti@artov.ism.cnr.it

7 National Research Nuclear University MEPhI, Kashirskoe Sh. 31, 115409 Moscow, Russia

8 P.N. Lebedev Physical Institute, Russian Academy of Sciences (RAS), Leninsky Pr. 53, 119991 Moscow, Russia

9 School of Science and Technology, Physics Division, Università degli studi di Camerino, via Madonna delle Carceri, 62032 Camerino, Italy; andrea.dicicco@unicam.it (A.D.C.); roberto.gunnella@unicam.it (R.G.); marco.minicucci@unicam.it (M.M.); angela.trapananti@unicam.it (A.T.)

10 Center for Life Nano Science @Sapienza, Istituto Italiano di Tecnologia, 00161 Rome, Italy

11 Dipartimento di Scienze di Base e Applicate per l'Ingegneria, Università degli studi di Roma "La Sapienza" Roma, 00161 Rome, Italy

12 Elettra-Sincrotrone Trieste, Area Science Park, 34149 Trieste, Italy; lucagiannessi@gmail.com (L.G.); claudio.masciovecchio@elettra.eu (C.M.)

13 ENEA C.R. Frascati, Via E. Fermi 45, 00044 Frascati RM, Italy

14 National Scientific and Technical Research Council, C1425FQB Buenos Aires, Argentina; newjuanjo@gmail.com (J.J.L.); jorobledo@unc.edu.ar (J.I.R.); jsan@famaf.unc.edu.ar (H.J.S.)

15 Istituto Nazionale di Fisica Nucleare (INFN) Sezione di Roma La Sapienza, P.le Aldo Moro 2, 00185 Rome, Italy

16 Istituto di Struttura della Materia (ISM)-Consiglio Nazionale delle Ricerche (CNR), Division of Ultrafast Processes in Materials (FLASHit), Area della Ricerca di Roma 1, Via Salaria Km 29.3, I-00016 Monterotondo Scalo, Italy

[17] Centro Fermi—Museo Storico della Fisica e Centro Studi e Ricerche "Enrico Fermi", 00184 Rome, Italy
[18] Faculty of Mathematics Astronomy Physics, National University of Córdoba, Córdoba X5000GYA, Argentina
* Correspondence: francesco.stellato@roma2.infn.it

Received: 31 January 2019; Accepted: 2 March 2019; Published: 7 March 2019

Abstract: A proposal for building a Free Electron Laser, EuPRAXIA@SPARC_LAB, at the Laboratori Nazionali di Frascati, is at present under consideration. This FEL facility will provide a unique combination of a high brightness GeV-range electron beam generated in a X-band RF linac, a 0.5 PW-class laser system and the first FEL source driven by a plasma accelerator. The FEL will produce ultra-bright pulses, with up to 10^{12} photons/pulse, femtosecond timescale and wavelength down to 3 nm, which lies in the so called "water window". The experimental activity will be focused on the realization of a plasma driven short wavelength FEL able to provide high-quality photons for a user beamline. In this paper, we describe the main classes of experiments that will be performed at the facility, including coherent diffraction imaging, soft X-ray absorption spectroscopy, Raman spectroscopy, Resonant Inelastic X-ray Scattering and photofragmentation measurements. These techniques will allow studying a variety of samples, both biological and inorganic, providing information about their structure and dynamical behavior. In this context, the possibility of inducing changes in samples via pump pulses leading to the stimulation of chemical reactions or the generation of coherent excitations would tremendously benefit from pulses in the soft X-ray region. High power synchronized optical lasers and a TeraHertz radiation source will indeed be made available for THz and pump–probe experiments and a split-and-delay station will allow performing XUV-XUV pump–probe experiments.

Keywords: free electron lasers; coherent imaging; X-ray Raman; X-ray absorption; THz radiation

1. Introduction

The advent of Free Electron Lasers (FELs) opened up the way to an unprecedented, wide class of experiments exploiting the peculiar features of these radiation sources. Key elements are the high peak brilliance that can be higher than 10^{27} photons/(s mm^2 mrad^2 0.1% bandwidth) and the short pulse duration, which is of the order of tens of femtoseconds. FELs can therefore allow high time resolution measurements and may provide a high signal-to-noise ratio. By exploiting the high peak brilliance and the extremely short FEL pulses the so-called diffract-and-destroy regime, in which interpretable data are gathered before the sample is destroyed by the FEL pulse radiation [1], can be explored, overcoming one of the main limitations of synchrotron radiation based experiments, namely sample radiation damage. This idea has been proven in several experiments on various samples, both biological [1–6] and non-biological [7], at different wavelengths ranging from the UV to the hard X-rays region. Actually, this issue is particularly relevant since coherent diffraction imaging (CDI) of biological system using conventional methods is ultimately limited by radiation damage owing to the large amount of energy deposited in the sample by the photon beam [7,8].

The unique FEL features (energy range, time resolution and brilliance) can be exploited in several branches of physics, chemistry, material science and biology. In this paper, we describe the main experimental lines that can be investigated at the EuPRAXIA@SPARC_LAB FEL [9,10] (Figure 1). The EuPRAXIA@SPARC_LAB FEL will provide photon pulses with high intensity, up to 10^{12} photons/pulse, down to a wavelength of about 3 nm, in the so called "water window". The foreseen pulse energy will reach 180 μJ and the bandwidth will range between 0.4% and 0.9%, according to the machine operation scheme. The pulse length will be of tens of femtoseconds. The experimental activity will be focused on the realization of a plasma driven short wavelength FEL and the first expected FEL operational mode will be based on the self amplification of spontaneous radiation (SASE) mechanism with tapered undulators. Details about foreseen beam parameters are given in [9]. The facility will also provide a high-power (0.5 PW) laser system and a TeraHertz (THz) radiation source. These sources will allow performing laser pump–FEL probe and THz pump–FEL probe experiments. Moreover, a split-and-delay element will allow laser pump–FEL probe experiments. A fully equipped experimental endstation designed to perform this variety of experiments will be designed and built. The experimental hall will be designed in order to allow the highest flexibility, optimizing the available space to perform a wide class of experiments (see Figure 2). All the aspects of the experimental needs will be considered, therefore next to the experimental hall a large space for the support to the experimental activities, but also for rest breaks of people working on the experiments, will be available.

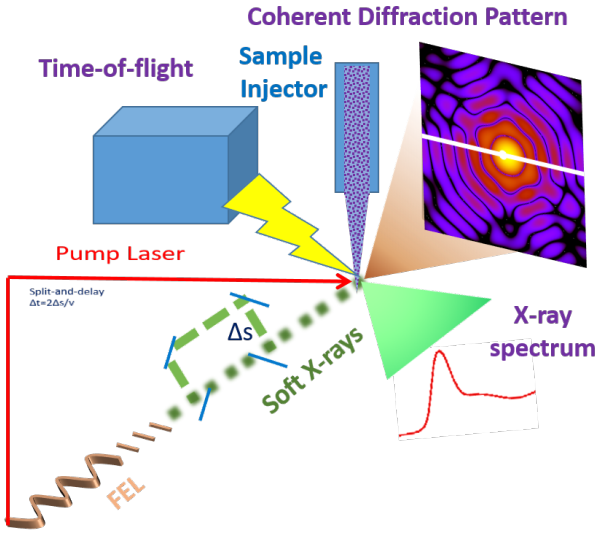

Figure 1. A simplified layout of the experiments that will be performed at EX-TRIM.

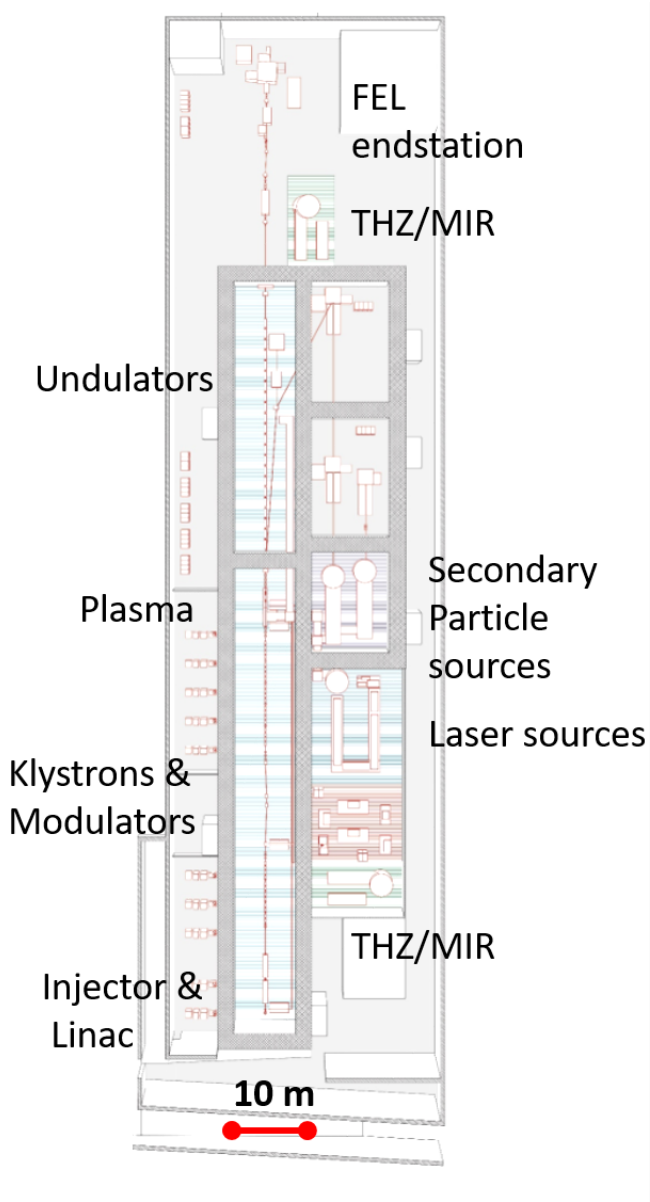

Figure 2. A layout of EuPRAXIA@SPARC_LAB. The building will be about 135 m long and 35 m wide. The location of the injector and linac, of the klystrons, of the plasma module and of undulators is shown on the left side. The location of the two THz/MIR and of the FEL endstation is highlighted on the right side.

2. Expected Results

In this section, we present and discuss some of the results that we expect to be able to obtain owing to the peculiar features of the EuPRAXIA@SPARC_LAB facility.

2.1. Coherent Imaging of Biological Samples

FEL radiation can be used to gather information on several kinds of biological samples. Biological single particle imaging is one of the main topics of FEL research with dedicated beamlines, although the FEL intensity, the available detectors, and techniques to introduce the sample into the

focused X-ray sampling position, were all insufficient to obtain (near) atomic resolution structural information from single biological macromolecules [11]. Nevertheless, recent experiments performed at LCLS showed that single-shot diffraction patterns from biological samples as small as 70 nm in diameter (e.g., the enterobacteria phage PR772 [12,13]) can be measured, and still at LCLS signal up to 5.9Åresolution was observed from rice dwarf virus [14]. Measurements performed at SACLA allowed recovering the electron density of chloroplast with 70 nm resolution [15]. Dataset of coherent imaging patterns have also been made available for the scientific community [16,17]. In the specific case at hand here, thanks to the photon energy range delivered by the EuPRAXIA@SPARC_LAB FEL, coherent imaging experiments in the water window will allow obtaining structural information on cells, organelles, viruses and protein aggregates [3–5,18] by performing measurements at room temperature and with samples staying in their native state. Exploiting the high degree of transverse coherence of the EuPRAXIA@SPARC_LAB FEL beam, which is foreseen to be between 80% and 100%, 2D images of a variety of biological samples, including bacteria (see Figure 3a), viruses (see Figure 3b), cells, cell organelles and protein aggregates and fibrils [19,20], can be obtained. The possibility of obtaining high resolution structures of fibrils in native conditions is particularly relevant to study the dynamics of their formation, which is important for both industrial/pharmaceutical [21,22] and bio-medical [20] applications. When dealing with a class of identical objects (e.g., viruses or ribosomes), it is also possible to combine the diffraction patterns, coming from different FEL pulses hitting different elements of the class, to get a full 3D reconstruction [23].

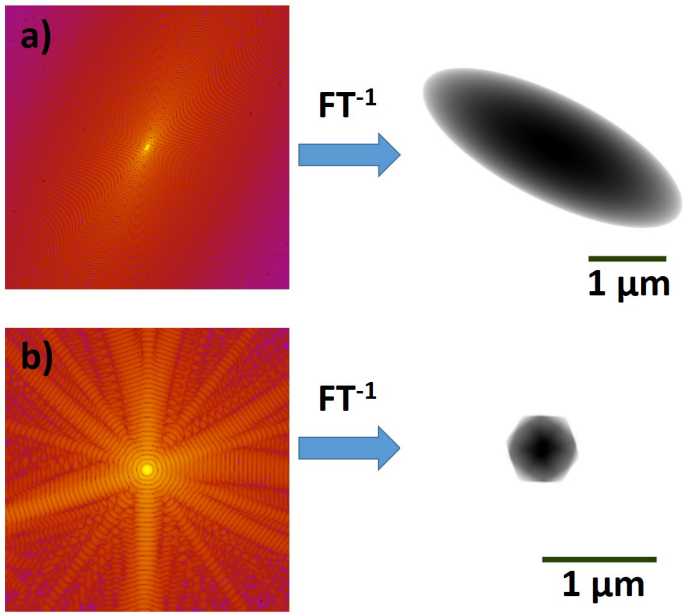

Figure 3. Simulated data for coherent imaging experiments at the EuPRAXIA@SPARC_LAB FEL. (**a**) A simulated diffraction pattern and the reconstruction of the electron density of a 2 µm long spheroid, with a shape similar to that of an elongated bacterium. (**b**) A simulated diffraction pattern from a 600 nm diameter icosahedral virus. Simulations were performed using the software Condor [24] assuming a Gaussian-shaped beam with a diameter of 3 µm, a wavelength of 2.87 nm and a pulse intensity of 100 µJ, which is, according to simulations, the expected pulse energy delivered on the sample by an EuPRAXIA@SPARC_LAB pulse.

The attainable resolution depends on the sample's composition and size and it is limited by FEL wavelength and photon brilliance, but, thanks to the high contrast associated to the water-window energy

range, the EuPRAXIA@SPARC_LAB will be a suitable facility to perform CXI measurements on a wide class of biological objects. It is worth pointing out that, when dealing with biological samples, which are mainly composed by light atoms and preferentially live in a water environment, there is a particular interest in performing measurement in the so-called water window, i.e., the energy range between carbon (282 eV) and oxygen (533 eV) K-edge. In this range, the absorption contrast between the carbon of organelles and the water of both cytoplasm and the liquid surrounding the cell is quite high. For this reason, the EuPRAXIA@SPARC_LAB will be particularly suitable to perform high-contrast imaging experiments on biological samples in their living, hydrated, native state, without the need of cooling or staining them, as is the case for other microscopy techniques such as electron microscopy.

2.2. Time-Resolved X-ray Absorption Spectroscopy in the Water Window

Besides imaging experiments, which typically require single wavelength pulses, spectroscopy experiments requiring the scan of a (limited) energy range can also be performed at a FEL.

The main advantage of performing XAS experiments at the EuPRAXIA@SPARC_LAB FEL with respect to the more compact HGG sources (as, for example, those described in [25]) is the number of photons per pulse, which is foreseen to be as high as 10^{12} photons/pulse, thus being still significantly higher than that currently achievable at HGG sources (e.g., Popmintchev et al. [26] reported a fux of more than 10^9 photons/second in the water window energy range). The high intensity of the FEL pulses will allow acquiring data with a good signal-to-noise ratio from single-shots measurements.

In this context, X-ray Absorption Spectroscopy (XAS) can be used as a tool to directly observe the molecular structure during chemical dynamics studies [27,28]. Real time observations require indeed fast time and small spatial resolutions, which can be guaranteed by the short, intense EuPRAXIA@SPARC_LAB FEL pulses. In particular, either by tuning the undulators to the appropriate energy, or exploiting the natural jitter of the FEL radiation generated in SASE mode, the experiments performed at EuPRAXIA@SPARC_LAB will allow measuring the informative, low-energy portion of the XAS spectrum, the so-called XANES (X-ray Absorption Near Edge Spectroscopy) region. Quantitative analysis tools of XANES data are nowadays available [29,30] including those based on first principles calculations [31–33]. Therefore, FEL-XAS measurements will become a powerful tool to provide unique information on the local geometry, electron density and spin states around selected atomic moieties [34]. Soft X-rays as the ones that will be produced by EuPRAXIA@SPARC_LAB are well suited for chemical and biological studies in the water window region. This region includes the K edge of elements such as C, N and O, and the L edge of 3d transition metals, which are of interest in many biologically relevant cases [35,36].

Examples of pioneering soft X-ray L-edge FEL-XAS transmission experiments include measurements of Al, Ge and Ti thin films for variable fluence (see, for example, [37–39]). In those experiments, ultrafast electron heating pumping matter at extremely high temperatures, as well as saturable absorption effects were observed. FEL experiments were found to be extremely useful to explore highly uniform warm dense matter (WDM) conditions, a regime exceedingly difficult to reach in present laboratory studies, but relevant to various fields, including high-pressure and planetary science, astrophysics, and plasma production. Various FEL-based ultrafast techniques can be used to probe WDM properties at electron temperatures in the 1–10 eV range and beyond. Those previous results naturally call for further challenging experiments at the EuPRAXIA@SPARC_LAB FEL as well as for parallel developments of suitable interpretation schemes for modeling and understanding the X-ray absorption cross section under high-fluence conditions (see [40] and refs. therein).

For experiments near the chemically relevant carbon K edge at 284.2 eV, the EuPRAXIA@SPARC_LAB FEL can be used to study dissociation reactions of molecular cations, that until today could not been resolved in time, using transient absorption at the carbon K-edge. Moreover, XAS measurements at the

L-edge of 3d transition metals provides unique information on the local metal charge and spin states by directly probing 3d-derived molecular orbitals through 2p-3d transitions. However, this soft X-ray technique has been rarely used at synchrotron facilities for mechanistic studies of metalloenzymes due to the problems with X-ray-induced sample damage and strong background signals from light elements that can dominate the low metal signal. It has been recently shown [34] that Mn L-edge absorption spectra can be collected at room temperature at a FEL. This paves the way for future structural and dynamical studies of metalloenzymes exploiting soft X-ray FEL radiation such as the one produced by EuPRAXIA@SPARC_LAB.

2.3. Time-Resolved Coherent Raman Experiments with X-ray Pulses

One of the most intriguing challenges in modern scientific research is the capability of monitoring transient atomic motions that govern physical, chemical and biological phenomena, measuring structural molecular changes of reacting species over few Ångstrom lengths on sub-picosecond timescales. The standard approach used to investigate structural dynamics is the pump–probe scheme, in which light pulses are used to first excite (pump) and subsequently interrogate (probe) a system [41]. The use of intense, ultra-short, soft X-ray radiation pulses such as those generated by the EuPRAXIA@SPARC_LAB FEL would tremendously benefit pump–probe investigations, whereof two different situations will be addressed: on the one hand, X-ray pulses can be exploited as pump pulse for stimulating chemical reactions or for generating coherent excitations, and, on the other hand, they can be used as selective probe to monitor the evolution from reactant to photoproduct.

Raman spectroscopy is a very powerful experimental tool for the detection of molecular vibrations, which are related to the force constant between atoms. In this scenario, accessing the Raman spectrum during and upon the FEL interaction would disclose any vibrational and structural modification occurring on the system under investigation. The subsequent electronic relaxation modifies the force field, generating a fragmentation of the molecule. To follow the evolution from the point of view of molecular vibrations, two crucial requirements are needed: (1) collimated signal, to avoid the luminescence background generated from the sample after the FEL interaction; and (2) sub-picosecond time resolution to follow the fragmentation process. Therefore, spontaneous Raman spectroscopies are ineffective in this exploration, due to the isotropic signal and temporal resolution [42], compromised by the fundamental restrictions dictated by the Fourier transform limit. Femtosecond stimulated Raman scattering (FSRS) is a recently developed technique [43–47], in which a femtosecond actinic pulse (AP) initiates the photochemistry of interest. The system is subsequently interrogated by a pair of overlapped pulses: the joint presence of a broadband ultrashort probe pulse (PP) and a narrowband picosecond Raman pulse (RP) induces vibrational coherences which are read out as heterodyne coherent Raman signals [48,49]. Notably, the probed Raman features are engraved onto the highly directional PP, and, hence, SRS provides an efficient suppression of the incoherent fluorescence background. Moreover, thanks to the different temporal and spectral properties of the pulses, femtosecond SRS represents an ideal tool to study structural changes in ultrafast photophysical and photochemical processes, providing both femtosecond time precision and high spectral resolution [45,50–52]. The narrowband RP can be generated from a two-stage optical parametric amplifier that produces tunable infrared-visible pulses, followed by spectral compression via frequency doubling in a 25 mm beta-barium borate crystal [53]. The femtosecond AP, so far in the visible spectral region, can be replaced with XUV-FEL. In this way, tuning the soft X-ray wavelength in resonance with a specific atomic absorption edge, it would be possible to selectively excite specific atoms and follow the temporal evolution of Raman mode disappearance, which depends on atomic role in molecular oscillation and the electronic coupling between atoms. From another perspective, pulses in the X-ray domain, resonant with valence excited-state transitions, can be used as probe pulses in Raman based spectroscopies, enabling

to selectively isolate contributions from specific sites of molecular moieties. In particular, combining an X-ray femtosecond probe pulse, with a visible photochemical pump pulse, would give the chance to perform X-ray Impulsive Vibrational Scattering (X-IVS), in which a visible pump pulse, besides triggering a photo-reaction, stimulates vibrational coherences on the system, modulating the transmission of a temporally delayed XUV probe, at the frequencies of the coherently activated vibrations [54,55]. For this reason, recording the transmission of the probe pulse enables real-time monitoring of Raman active modes. Fourier transforming the detected signal over the temporal delay between pump and probe recovers the transient Raman spectrum of the system under investigation. While IVS has been extensively exploited in the visible spectral region for probing ground and excited state coherences on both molecular and solid-state compounds [56,57], its potential in the X-ray domain is still an unexplored territory, which can be disclosed thanks to the EuPRAXIA@SPARC_LAB FEL experimental endstation. Notably, in close analogy with the atomic selectivity achieved by using a XUV pump pulse, employing a probe pulse resonant with a specific electronic transition absorption edge would provide the chance of isolating coherent atomic motions involving only the desired atomic moieties. A schematic view of a pump–probe Raman experiment is depicted in Figure 4.

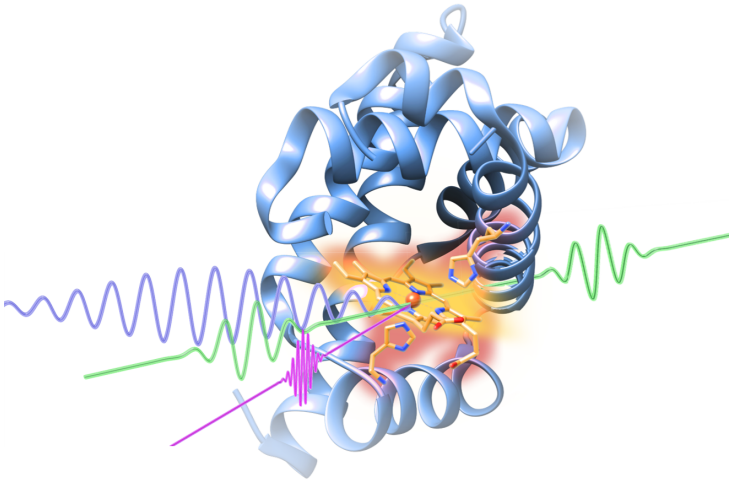

Figure 4. Schematic view of a time-resolved (pump–probe) Raman experiment on a protein.

Further development will be done in the field of localized dynamic studies by nano-Raman instruments. Both apertureless and fiber-based Scanning Near-field Optical Microscopy (SNOM) will be used to increase the lateral spatial resolution in the tens of nm: in this case, the excitation of the sample is kept as uniform as possible, and collection of scattered signal from local spot on the sample is conducted [58,59].

Another field where one can exploit the XUV photons generated by the EuPRAXIA@SPARC_LAB FEL is the study by means of coherent electronic Raman process [39] of photo-induced chemical processes represented by the detection of electronic coherences (based on a composite X-ray pulse sequence) generated during the system dynamics [60]. For example, within such a scheme, a combination of short, soft X-ray FEL pulses can be used to directly detect the passage through conical intersections (CIs). Notably, the photoinduced excited state dynamics of polyatomic molecules is often dominated by CI, regions of degeneracy between two or more electronic surfaces [61]. The dynamical behavior of molecules in the vicinity of CIs dictates the resulting photophysics and photochemistry of the molecule. Given the ubiquity and importance of CIs in all photoinduced processes, from solar energy conversion to vision,

finding a direct, experimental observable of the dynamics through a CI would be a significant development in our understanding of excited state photo-induced dynamics.

2.4. Photo-Fragmentation of Molecules

Another kind of applications that would largely benefit from the peculiar features of the EuPRAXIA@SPARC_LAB FEL radiation is represented by the wide class of experiments aimed at studying the interaction of intense radiation pulses with molecules. How organic and biological molecules redistribute the energy of absorbed light is indeed a key fundamental question in organic chemistry and biology which time-resolved experiment can help to settle [62–67]. This class of experiments will help understanding the basic mechanisms of photo-protection/damage of amino acids [68], proteins and DNA/RNA [69]. XUV or X-rays pump laser pulses of low intensity with a few femtoseconds duration contain photons ranging up to hundreds of eV. Single-photon ionization is a dominant absorption channel triggering the ultrafast charge migration process in the parent cation. Probing the resulting non-equilibrium dynamics using short, intense pulses such as those produced by the EuPRAXIA@SPARC_LAB FEL at delays varying on the femtosecond timescale allows resolving in real-time the electron density through time-resolved imaging [70–74].

An example of what can be seen in a photo-fragmentation experiment as it will be implemented at EuPRAXIA@SPARC_LAB FEL is given in Figure 5. In particular, we display the real-space distribution of the molecular charge at six representative times of the phenylalanine amino acid after illumination with an ionizing XUV 300-as pulse.

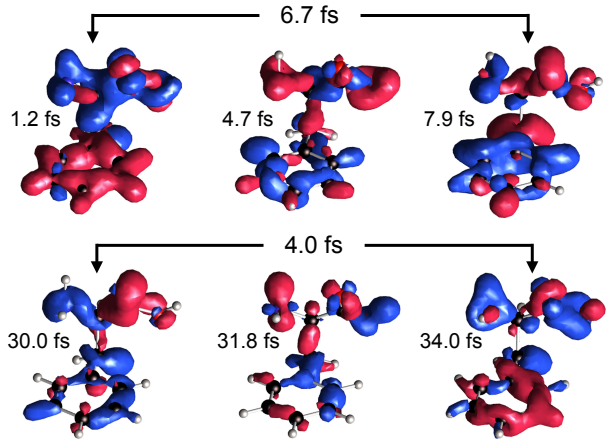

Figure 5. Real-space distribution of the molecular charge at six representative times of the phenylalanine amino acid after illumination with an ionizing XUV 300-as pulse. The figure is taken from Reference [68] (Copyright 2018 by the American Chemical Society).

2.5. Resonant Inelastic X-ray Scattering

In atomic inner shell spectroscopy, spectra can show peculiar characteristics associated with a variety of different scattering interactions. When atoms are irradiated with incident energy lower but close to an absorption edge, scattering peaks appear due to an inelastic process known as Resonant Inelastic X-ray Scattering (RIXS) or X-ray Resonant Raman Scattering [75]. These RIXS peaks display typical features, such as a characteristic long-tail spreading to the region of lower energy. This scattering process is a high demanding photon flux. In general, RIXS experiments are carried out at synchrotron facilities using high-resolution spectrometers for detecting the scattering signal. Nevertheless, in recent years, RIXS has

been observed using an Energy Dispersive Setup (EDS) with synchrotron radiation. The analysis of the collected signal shows that hidden on the peak tails there is valuable information about the chemical environment of the atom under study [76]. During the last decade, several works have been published showing the first applications of a novel RIXS tool (named EDIXS) for the discrimination, determination and characterization of chemical environments in a variety of samples and irradiation geometries and even combined with other spectroscopic techniques [76–86]. Due to its versatility, EDIXS was applied in the typical 45°–45° setup for inspection of the material bulk, in total reflection for the study of the most external atomic layers of a sample, in grazing incidence used for depth resolved chemical speciation analysis and even in confocal setup to obtain chemical state information in a 3D regime, reaching nanometric spatial resolution. Owing to the EDIXS high sensitivity, this technique can be extended to the study of local chemical environments with applications in many field of science, as geology, chemistry, physics, material science and industry, etc., where a precise quantification of different compounds is required [79]. This methodology is fast, reliable and straightforward. It has several benefits compared with other spectroscopic techniques, such as fast acquisition, low self-absorption and the avoidance of any energy scan during the measurements. A remarkable field of application of EDIXS is in the context of pulsed X-ray sources, e.g., FELs. Besides the application of EDIXS for fast structural characterization of materials, this tool allows time-resolved investigations of a variety of atomic processes and of the dynamics of samples of interest exposed, for example, to changing conditions of temperature, atmosphere, pressure, etc. Previous results regarding time-resolved discrimination of chemical environments [80] have showed time resolution of the order of the second when monochromatic synchrotron radiation was used (flux $\sim 10^8$ ph/s). Due to the higher FEL photon flux, we expect to obtaining sub-second, and even millisecond, time-resolved experiments when a FEL source is used. This kind of (very) fast characterizations are currently impossible to achieve by conventional methods. Even non-conventional sources (storage rings) employing traditional techniques for atomic environment analysis (EXAFS, XANES, etc.) are useless in time-resolved spectroscopy because of the need of energy scan. This limitation establishes an ultimate frontier for these techniques that cannot be overcome during time dependent measurements. At this point, the one-shot character of EDIXS makes a crucial difference in favor of it. There are a variety of relevant cases to study with time-resolved EDIXS, both in basic research and in applications to the industry and technology fields. As for the multiple applications of time-resolved EDIXS using the EuPRAXIA@SPARC_LAB FEL (with produces photons with a maximum energy of ∼415 eV) as basic research, we mention the analysis of nitrogen and carbon states in the evolution of biological systems, for example in the study of the role of nitrogen during photosynthesis and of the chemical state of carbon during cell divisions. Concerning technological and industrial applications, a wide range of opportunities exists, since carbon plays a role in many situations. Just to mention a few of them: diamond structural variations under high conditions of pressure or graphene and complex carbon structures reactions to external excitations. The key element at the basis of the feasibility of all the RIXS experiments we have illustrated is the combination of a fast time resolution technique with the EuPRAXIA@SPARC_LAB source, delivering extremely high photon fluxes.

2.6. THz/MIR Sources

The interest in THz radiation is recognized since many years for its potential to advance research in several scientific fields. In addition, THz research has many industrial prospects, so that THz activities may offer potential spin-off not only associated to condensed matter basic research, e.g., semiconductor and superconductors materials, whose characterization may have a direct impact on many technologies, but also in R&D of detectors and imaging. A great expectation for industry is the development of imaging for biomedical applications and security issues.

THz radiation lies between the photonic and the electronic bands of the electromagnetic spectrum, and it extends from 300 GHz up to 10 THz. THz is non-ionizing and highly penetrating in a large variety of dielectric materials, e.g., plastic, ceramics, and paper. The wavelength of the THz radiation is of the order of many important physical, chemical and biological processes (see Figure 6), including superconducting gaps, exotic electronic transitions and protein dynamical processes. The THz part of the spectrum is energetically equivalent to many important physical, chemical and biological processes including superconducting gaps, exotic electronic transitions and protein dynamical processes. Recently, a new generation of sources, based on particle accelerators, allows increasing the average and peak power, by many orders of magnitude, and extends the spectral range up to the Mid-Infrared (100 THz, Middle-InfraRed (MIR)), making the whole spectral region accessible to different frequency- and time-domain experiments. Indeed, a linac-driven THz/MIR source can deliver broadband pulses with femtosecond shaping, and with the possibility to store a high energy in a single pulse [87]. In addition, taking advantage of electron beam manipulation techniques, high power, narrow-band radiation can be also generated [88]. Finally, high brightness electron beams also permit the possibility to extend the emission towards the MIR, having a unique source covering three decades in wavelength from 1000 microns to 1 micron. This provides a unique chance to realize THz/MIR-pump/THz/MIR probe spectroscopy, a technique essentially unexplored up to now.

The potential of THz and MIR frequency and time domains spectroscopies are displayed in Figure 6, where we show a not exhaustive review of excitations whose characteristic energy are in resonance with those of specific processes.

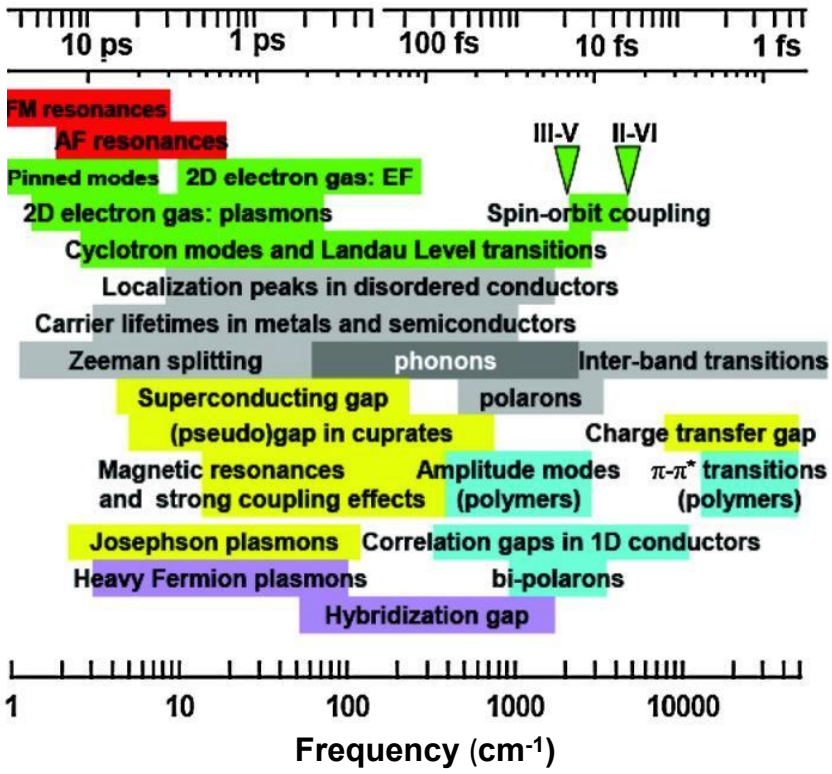

Figure 6. Frequency and time domain of THz/MIR spectroscopy.

An electromagnetic source can be characterized in terms of time duration, field strength, pulse shape, bandwidth and frequency. Their choice depends on the class of experiments of interest. An effective

THz/MIR source should have higher peak fields, from 100 kV/cm to 50 MV/cm, the coverage of a spectral range up to a frequency of 100 THz, a full pulse shaping and a sub-ps duration. The THz/MIR source at EuPRAXIA@SPARC_LAB will be designed to achieve these requirements.

THz/MIR radiation will be generated at EuPRAXIA@SPARC_LAB through different production schemes based on ultra-short, i.e., ≈10–100 fs, electron bunches. Two beam lines are considered in the first phase of the EuPRAXIA@SPARC_LAB project: one at low energy, i.e., 30–50 MeV, and the second one at higher energy, i.e., 1 GeV, in proximity of the FEL extraction site (see Figure 2).

Being produced by the same electron beam, these two sources are naturally synchronized on few femtosecond time scales. To perform THz pump X-ray probe experiments, we plan to take advantage of laser-based THz streaking, which effectively phase-locks a single-cycle THz pulse to the X-ray pulse. This technique simultaneously clocks the arrival time of the two sources and allows the measurement of the X-ray pulse temporal profile with a precision of tens of femtoseconds.

The first beamline, consisting of a THz/MIR SASE FEL able to emit quasi-monochromatic and fully polarized (with variable polarization), radiation from THz to MIR, will be optimized for experiments involving high peak power and narrow band THz/MIR radiation. The second beamline will combine the Coherent Diffraction Radiation [89], emitted from a rectangular slit in a metallic screen, to the VUV/X SASE FEL radiation to perform THz pump X-ray probe experiments.

Coherent Transition and Diffraction Radiation (CTR and CDR, respectively) are the chosen production mechanisms at high electron beam energy, i.e., ∼GeV scale, with the advantage of a broadband spectrum up to several THz depending on how short the bunch duration is. In the case of CDR, a further advantage is represented by the non-disruptiveness for the electron beam [90]. Both electron and THz representative radiation parameters are reported in Table 1.

Table 1. Electron beam and THz source parameters from CDR.

Beam Parameters		**Source Parameters**	
E (GeV)	1	Frequency (THz)	0.3–10
Q (pC)	200	P_{peak} (MW)	>100
σ_z (μm)	30	E_{ph} (μJ)	≈100

At low electron beam energy, around 30 and 50 MeV, a SASE FEL operating in the MIR/THz range has been considered for the generation of highly intense narrow band, tunable radiation. A SPARC-like undulator [91] (2.8 cm period, K parameter ($K = \frac{eB_0\lambda_u}{2\pi mc}$, with B_0 the magnetic field on axis and λ_u the undulator period; e and m are the electron charge and mass, and c the speed of light in vacuum) of 1.2) with variable gap has been considered for the calculation of MIR/THz radiation based on GPT simulations [92] for the electron beam dynamics and Ming Xie formulas [93] for the SASE FEL performances; saturation occurs within 5 m of undulator length. Both electron beam and MIR/THz radiation parameters are listed in Table 2.

Table 2. Electron beam and MIR/THz source parameters from a MIR SASE FEL.

Beam Parameters		**Source Parameters**	
E (MeV)	30–50	λ_r (μm)	10–3
Q (pC)	200	L_{sat}	3–4.4
σ_z (μm)	50	P_{sat} (MW)	140–135
I_{peak} (kA)	480	N_{ph}	$\sim 10^{15}$
$\Delta E/E$ (%)	0.1–0.4	E_{ph} (μJ)	∼60

The magnetic structure of the undulator will be optimized to provide fully polarized light. The polarization can be modfied from linear, circular, elliptical, to more complex structures such as helicoidal polarization. These polarization states, which are absolutely unconventional for THz and MIR lights and of difficult realization with thermal- and laser-based sources, will provide the possibility to pump exotic modes such as skyrmions in magnetic systems, Weyl and Dirac fermions [94] in non-trivial quantum matter, and Higgs and Legett modes in multi-gap superconductors and charge-density wave materials. Experiments in which all phonon modes of exotic systems can be selectively pumped will be also accessible, opening the possibility to control the lattice structure on the ps-scale and, consequently, to modulate the electronic ground state of the systems [95]. Localized dinamical spectroscopic imaging will be performed by THz apertureless-SNOM, where the tip's antenna function will allow performing imaging with a lateral resolution well below 1 micron [96].

3. Discussion and Conclusions

In this paper, we summarize the main experimental lines of investigation that can be implemented at the EuPRAXIA@SPARC_LAB FEL exploiting its ultra-short, bright FEL pulses generated in the "water-window". The realization of the EuPRAXIA@SPARC_LAB infrastructure will allow INFN to consolidate a strong scientific, technological and industrial role in a competing international context. To exploit at best the features of this compact machine, a great effort will have to be addressed in developing, designing and assembling all the optical components necessary to deliver the FEL photons to the user endstation and in developing and characterizing detectors able to optimize the signal-to-noise ratio for all the foreseen classes of experiments. We are confident that the EuPRAXIA@SPARC_LAB photon source, with its multi-purpose beamline, designed and equipped to perform the classes of experiments highlighted in this paper, will be highly beneficial for the national and international community of FEL radiation users.

Author Contributions: Conceptualization, writing—review and editing, all authors; and Writing—original draft preparation, all authors.

Funding: This research was funded by European Union's Horizon 2020 research and innovation programme under grant agreement No. 653782. One of the authors (S.D.) acknowledges the support by the Competitiveness Program of NRNU MEPhI (Moscow).

Conflicts of Interest: The authors declare no conflict of interest.

Abbreviations

The following abbreviations are used in this manuscript:

AP	Actinic Pulse
CDI	Coherent Diffraction Imaging
CDR	Coherent Diffraction Radiation
CTR	Coherent Transition Radiation
CI	Conical Intersection
EDS	Energy Dispersive Setup
FEL	Free Electron Laser
FSRS	Femtosecond stimulated Raman scattering
MIR	Middle-InfraRed
PP	Probe Pulse
RIXS	Resonant Inelastic X-ray Scattering
RP	Raman Pulse

SASE	Self Amplification of SpontanEous radiation
SNOM	Scanning Near-field Optical Microscopy
THz	Tera Hertz
XAS	X-ray Absortpion Spectroscopy
X-RIVS	X-ray Impulsive Vibrational Scattering
XUV	eXtreme Ultra Violet

References

1. Chapman, H.N.; Fromme, P.; Barty, A.; White, T.A.; Kirian, R.A.; Aquila, A.; Hunter, M.S.; Schulz, J.; DePonte, D.P.; Weierstall, U.; et al. Femtosecond X-ray protein nanocrystallography. *Nature* **2011**, *470*, 73–77. [CrossRef] [PubMed]
2. Boutet, S.; Lomb, L.; Williams, G.J.; Barends, T.R.; Aquila, A.; Doak, R.B.; Weierstall, U.; DePonte, D.P.; Steinbrener, J.; Shoeman, R.L.; et al. High-resolution protein structure determination by serial femtosecond crystallography. *Science* **2012**, *337*, 362–364. [CrossRef] [PubMed]
3. Seibert, M.M.; Ekeberg, T.; Maia, F.R.; Svenda, M.; Andreasson, J.; Jönsson, O.; Odić, D.; Iwan, B.; Rocker, A.; Westphal, D.; et al. Single mimivirus particles intercepted and imaged with an X-ray laser. *Nature* **2011**, *470*, 78–81. [CrossRef] [PubMed]
4. Hantke, M.F.; Hasse, D.; Maia, F.R.; Ekeberg, T.; John, K.; Svenda, M.; Loh, N.D.; Martin, A.V.; Timneanu, N.; Larsson, D.S.; et al. High-throughput imaging of heterogeneous cell organelles with an X-ray laser. *Nat. Photonics* **2014**, *8*, 943–949. [CrossRef]
5. Van Der Schot, G.; Svenda, M.; Maia, F.R.; Hantke, M.; DePonte, D.P.; Seibert, M.M.; Aquila, A.; Schulz, J.; Kirian, R.; Liang, M.; et al. Imaging single cells in a beam of live cyanobacteria with an X-ray laser. *Nat. Commun.* **2015**, *6*, 5704. [CrossRef] [PubMed]
6. Fan, J.; Sun, Z.; Wang, Y.; Park, J.; Kim, S.; Gallagher-Jones, M.; Kim, Y.; Song, C.; Yao, S.; Zhang, J.; et al. Single-pulse enhanced coherent diffraction imaging of bacteria with an X-ray free-electron laser. *Sci. Rep.* **2016**, *6*, 34008. [CrossRef] [PubMed]
7. Henderson, R. The potential and limitations of neutrons, electrons and X-rays for atomic resolution microscopy of unstained biological molecules. *Q. Rev. Biophys.* **1995**, *28*, 171–193. [CrossRef] [PubMed]
8. Gutt, C.; Streit-Nierobisch, S.; Stadler, L.M.; Pfau, B.; Günther, C.; Könnecke, R.; Frömter, R.; Kobs, A.; Stickler, D.; Oepen, H.; et al. Single-pulse resonant magnetic scattering using a soft X-ray free-electron laser. *Phys. Rev. B* **2010**, *81*, 100401. [CrossRef]
9. Ferrario, M.; Alesini, D.; Anania, M.; Artioli, M.; Bacci, A.; Bartocci, S.; Bedogni, R.; Bellaveglia, M.; Biagioni, A.; Bisesto, F.; et al. EuPRAXIA@ SPARC_LAB Design study towards a compact FEL facility at LNF. *Nuclear Instrum. Methods Phys. Res. Sect. A* **2018**, *909*, 134–138. [CrossRef]
10. Villa, F.; Cianchi, A.; Coreno, M.; Dabagov, S.; Marcelli, A.; Minicozzi, V.; Morante, S.; Stellato, F. Design study of a photon beamline for a soft X-ray FEL driven by high gradient acceleration at EuPRAXIA@ SPARC_LAB. *Nuclear Instrum. Methods Phys. Res. Sect. A* **2018**, *909*, 294–297. [CrossRef]
11. Oberthür, D. Biological single-particle imaging using XFELs–towards the next resolution revolution. *IUCrJ* **2018**, *5*, 663. [CrossRef] [PubMed]
12. Reddy, H.K.; Yoon, C.H.; Aquila, A.; Awel, S.; Ayyer, K.; Barty, A.; Berntsen, P.; Bielecki, J.; Bobkov, S.; Bucher, M.; et al. Coherent soft X-ray diffraction imaging of coliphage PR772 at the Linac coherent light source. *Sci. Data* **2017**, *4*, 170079. [CrossRef] [PubMed]
13. Rose, M.; Bobkov, S.; Ayyer, K.; Kurta, R.P.; Dzhigaev, D.; Kim, Y.Y.; Morgan, A.J.; Yoon, C.H.; Westphal, D.; Bielecki, J.; et al. Single-particle imaging without symmetry constraints at an X-ray free-electron laser. *IUCrJ* **2018**, *5*, 727–736. [CrossRef] [PubMed]
14. Munke, A.; Andreasson, J.; Aquila, A.; Awel, S.; Ayyer, K.; Barty, A.; Bean, R.J.; Berntsen, P.; Bielecki, J.; Boutet, S.; et al. Coherent diffraction of single Rice Dwarf virus particles using hard X-rays at the Linac Coherent Light Source. *Sci. Data* **2016**, *3*, 160064. [CrossRef] [PubMed]

15. Takayama, Y.; Inui, Y.; Sekiguchi, Y.; Kobayashi, A.; Oroguchi, T.; Yamamoto, M.; Matsunaga, S.; Nakasako, M. Coherent X-ray diffraction imaging of chloroplasts from Cyanidioschyzon merolae by using X-ray free electron laser. *Plant Cell Physiol.* **2015**, *56*, 1272–1286. [CrossRef] [PubMed]
16. Van Der Schot, G.; Svenda, M.; Maia, F.R.; Hantke, M.F.; DePonte, D.P.; Seibert, M.M.; Aquila, A.; Schulz, J.; Kirian, R.A.; Liang, M.; et al. Open data set of live cyanobacterial cells imaged using an X-ray laser. *Sci. Data* **2016**, *3*, 160058. [CrossRef] [PubMed]
17. Hantke, M.F.; Hasse, D.; Ekeberg, T.; John, K.; Svenda, M.; Loh, D.; Martin, A.V.; Timneanu, N.; Larsson, D.S.; Van Der Schot, G.; et al. A data set from flash X-ray imaging of carboxysomes. *Sci. Data* **2016**, *3*, 160061. [CrossRef] [PubMed]
18. Ackermann, W.a.; Asova, G.; Ayvazyan, V.; Azima, A.; Baboi, N.; Bähr, J.; Balandin, V.; Beutner, B.; Brandt, A.; Bolzmann, A.; et al. Operation of a free-electron laser from the extreme ultraviolet to the water window. *Nat. Photonics* **2007**, *1*, 336. [CrossRef]
19. Popp, D.; Loh, N.D.; Zorgati, H.; Ghoshdastider, U.; Liow, L.T.; Ivanova, M.I.; Larsson, M.; DePonte, D.P.; Bean, R.; Beyerlein, K.R.; et al. Flow-aligned, single-shot fiber diffraction using a femtosecond X-ray free-electron laser. *Cytoskeleton* **2017**, *74*, 472–481. [CrossRef] [PubMed]
20. Stellato, F.; Fusco, Z.; Chiaraluce, R.; Consalvi, V.; Dinarelli, S.; Placidi, E.; Petrosino, M.; Rossi, G.; Minicozzi, V.; Morante, S. The effect of β-sheet breaker peptides on metal associated Amyloid-β peptide aggregation process. *Biophys. Chem.* **2017**, *229*, 110–114. [CrossRef] [PubMed]
21. Carbonaro, M.; Di Venere, A.; Filabozzi, A.; Maselli, P.; Minicozzi, V.; Morante, S.; Nicolai, E.; Nucara, A.; Placidi, E.; Stellato, F. Role of dietary antioxidant (-)-epicatechin in the development of β-lactoglobulin fibrils. *Biochim. Biophys. Acta* **2016**, *1864*, 766–772. [CrossRef] [PubMed]
22. Carbonaro, M.; Ripanti, F.; Filabozzi, A.; Minicozzi, V.; Stellato, F.; Placidi, E.; Morante, S.; Di Venere, A.; Nicolai, E.; Postorino, P.; et al. Human insulin fibrillogenesis in the presence of epigallocatechin gallate and melatonin: Structural insights from a biophysical approach. *Int. J. Biol. Macromol.* **2018**, *115*, 1157–1164. [CrossRef] [PubMed]
23. Ekeberg, T.; Svenda, M.; Abergel, C.; Maia, F.R.; Seltzer, V.; Claverie, J.M.; Hantke, M.; Jönsson, O.; Nettelblad, C.; Van Der Schot, G.; et al. Three-dimensional reconstruction of the giant mimivirus particle with an X-ray free-electron laser. *Phys. Rev. Lett.* **2015**, *114*, 098102. [CrossRef] [PubMed]
24. Hantke, M.F.; Ekeberg, T.; Maia, F.R. Condor: A simulation tool for flash X-ray imaging. *J. Appl. Crystallogr.* **2016**, *49*, 1356–1362. [CrossRef] [PubMed]
25. Pertot, Y.; Schmidt, C.; Matthews, M.; Chauvet, A.; Huppert, M.; Svoboda, V.; von Conta, A.; Tehlar, A.; Baykusheva, D.; Wolf, J.P.; et al. Time-resolved X-ray absorption spectroscopy with a water window high-harmonic source. *Science* **2017**, *355*, 264–267. [CrossRef] [PubMed]
26. Popmintchev, D.; Galloway, B.R.; Chen, M.C.; Dollar, F.; Mancuso, C.A.; Hankla, A.; Miaja-Avila, L.; O'Neil, G.; Shaw, J.M.; Fan, G.; et al. Near-and extended-edge X-ray-absorption fine-structure spectroscopy using ultrafast coherent high-order harmonic supercontinua. *Phys. Rev. Lett.* **2018**, *120*, 093002. [CrossRef] [PubMed]
27. Chergui, M.; Zewail, A.H. Electron and X-ray Methods of Ultrafast Structural Dynamics: Advances and Applications. *ChemPhysChem* **2009**, *10*, 28–43. [CrossRef] [PubMed]
28. Bressler, C.; Chergui, M. Molecular structural dynamics probed by ultrafast X-ray absorption spectroscopy. *Annu. Rev. Phys. Chem.* **2010**, *61*, 263–282. [CrossRef] [PubMed]
29. Benfatto, M.; Della Longa, S.; Natoli, C. The MXAN procedure: A new method for analysing the XANES spectra of metalloproteins to obtain structural quantitative information. *J. Synchrotron Radiat.* **2003**, *10*, 51–57. [CrossRef] [PubMed]
30. Bunau, O.; Joly, Y. Self-consistent aspects of X-ray absorption calculations. *J. Phys. Condens. Matter* **2009**, *21*, 345501. [CrossRef] [PubMed]
31. Rehr, J.J.; Kas, J.J.; Vila, F.D.; Prange, M.P.; Jorissen, K. Parameter-free calculations of X-ray spectra with FEFF9. *Phys. Chem. Chem. Phys.* **2010**, *12*, 5503–5513. [CrossRef] [PubMed]
32. La Penna, G.; Minicozzi, V.; Morante, S.; Rossi, G.; Stellato, F. A first-principle calculation of the XANES spectrum of Cu^{2+} in water. *J. Chem. Phys.* **2015**, *143*, 124508. [CrossRef] [PubMed]

33. Stellato, F.; Calandra, M.; D'Acapito, F.; De Santis, E.; La Penna, G.; Rossi, G.; Morante, S. Multi-scale theoretical approach to X-ray absorption spectra in disordered systems: An application to the study of Zn (II) in water. *Phys. Chem. Chem. Phys.* **2018**, *20*, 24775–24782. [CrossRef] [PubMed]
34. Kubin, M.; Kern, J.; Gul, S.; Kroll, T.; Chatterjee, R.; Löchel, H.; Fuller, F.D.; Sierra, R.G.; Quevedo, W.; Weniger, C.; et al. Soft X-ray absorption spectroscopy of metalloproteins and high-valent metal-complexes at room temperature using free-electron lasers. *Struct. Dyn.* **2017**, *4*, 054307. [CrossRef] [PubMed]
35. De Santis, E.; Minicozzi, V.; Proux, O.; Rossi, G.; Silva, K.I.; Lawless, M.J.; Stellato, F.; Saxena, S.; Morante, S. Cu (II)–Zn (II) Cross-Modulation in Amyloid–Beta Peptide Binding: An X-ray Absorption Spectroscopy Study. *J. Phys. Chem. B* **2015**, *119*, 15813–15820. [CrossRef] [PubMed]
36. De Santis, E.; Shardlow, E.; Stellato, F.; Proux, O.; Rossi, G.; Exley, C.; Morante, S. X-ray Absorption Spectroscopy Measurements of Cu-ProIAPP Complexes at Physiological Concentrations. *Condens. Matter* **2019**, *4*, 13. [CrossRef]
37. Nagler, B.; Zastrau, U.; Fäustlin, R.R.; Vinko, S.M.; Whitcher, T.; Nelson, A.; Sobierajski, R.; Krzywinski, J.; Chalupsky, J.; Abreu, E.; et al. Turning solid aluminium transparent by intense soft X-ray photoionization. *Nat. Phys.* **2009**, *5*, 693.
38. Di Cicco, A.; Hatada, K.; Giangrisostomi, E.; Gunnella, R.; Bencivenga, F.; Principi, E.; Masciovecchio, C.; Filipponi, A. Interplay of electron heating and saturable absorption in ultrafast extreme ultraviolet transmission of condensed matter. *Phys. Rev. B* **2014**, *90*, 220303. [CrossRef]
39. Principi, E.; Giangrisostomi, E.; Cucini, R.; Bencivenga, F.; Battistoni, A.; Gessini, A.; Mincigrucci, R.; Saito, M.; Di Fonzo, S.; D'Amico, F.; et al. Free electron laser-driven ultrafast rearrangement of the electronic structure in Ti. *Struct. Dyn.* **2016**, *3*, 023604. [CrossRef] [PubMed]
40. Hatada, K.; Di Cicco, A. Modeling Non-Equilibrium Dynamics and Saturable Absorption Induced by Free Electron Laser Radiation. *Appl. Sci.* **2017**, *7*, 814. [CrossRef]
41. Zewail, A.H. Femtochemistry. Past, present, and future. *Pure Appl. Chem.* **2000**, *72*, 2219–2231. [CrossRef]
42. Kruglik, S.G.; Jasaitis, A.; Hola, K.; Yamashita, T.; Liebl, U.; Martin, J.L.; Vos, M.H. Subpicosecond oxygen trapping in the heme pocket of the oxygen sensor FixL observed by time-resolved resonance Raman spectroscopy. *Proc. Natl. Acad. Sci. USA* **2007**, *104*, 7408–7413. [CrossRef] [PubMed]
43. Batignani, G.; Pontecorvo, E.; Ferrante, C.; Aschi, M.; Elles, C.G.; Scopigno, T. Visualizing Excited-State Dynamics of a Diaryl Thiophene: Femtosecond Stimulated Raman Scattering as a Probe of Conjugated Molecules. *J. Phys. Chem. Lett.* **2016**, *7*, 2981–2988. [CrossRef] [PubMed]
44. Batignani, G.; Bossini, D.; Di Palo, N.; Ferrante, C.; Pontecorvo, E.; Cerullo, G.; Kimel, A.; Scopigno, T. Probing ultrafast photo-induced dynamics of the exchange energy in a Heisenberg antiferromagnet. *Nat. Photonics* **2015**, *9*, 506. [CrossRef]
45. Dietze, D.R.; Mathies, R.A. Femtosecond stimulated Raman spectroscopy. *ChemPhysChem* **2016**, *17*, 1224–1251. [CrossRef] [PubMed]
46. Ferrante, C.; Pontecorvo, E.; Cerullo, G.; Vos, M.; Scopigno, T. Direct observation of subpicosecond vibrational dynamics in photoexcited myoglobin. *Nat. Chem.* **2016**, *8*, 1137. [CrossRef] [PubMed]
47. McCamant, D.W.; Kukura, P.; Yoon, S.; Mathies, R.A. Femtosecond broadband stimulated Raman spectroscopy: Apparatus and methods. *Rev. Sci. Instrum.* **2004**, *75*, 4971–4980. [CrossRef] [PubMed]
48. Yoshizawa, M.; Hattori, Y.; Kobayashi, T. Femtosecond time-resolved resonance Raman gain spectroscopy in polydiacetylene. *Phys. Rev. B* **1994**, *49*, 13259. [CrossRef]
49. Ferrante, C.; Batignani, G.; Fumero, G.; Pontecorvo, E.; Virga, A.; Montemiglio, L.; Cerullo, G.; Vos, M.; Scopigno, T. Resonant broadband stimulated Raman scattering in myoglobin. *J. Raman Spectrosc.* **2018**, *49*, 913–920. [CrossRef]
50. Fumero, G.; Batignani, G.; Dorfman, K.E.; Mukamel, S.; Scopigno, T. On the Resolution Limit of Femtosecond Stimulated Raman Spectroscopy: Modelling Fifth-Order Signals with Overlapping Pulses. *ChemPhysChem* **2015**, *16*, 3438–3443. [CrossRef] [PubMed]
51. Kukura, P.; McCamant, D.W.; Mathies, R.A. Femtosecond stimulated Raman spectroscopy. *Annu. Rev. Phys. Chem.* **2007**, *58*, 461–488. [CrossRef] [PubMed]

52. Batignani, G.; Fumero, G.; Pontecorvo, E.; Ferrante, C.; Mukamel, S.; Scopigno, T. Genuine dynamics vs. cross phase modulation artefacts in Femtosecond Stimulated Raman Spectroscopy. *ACS Photonics* **2019**, *6*, 492–500. [CrossRef]
53. Pontecorvo, E.; Kapetanaki, S.; Badioli, M.; Brida, D.; Marangoni, M.; Cerullo, G.; Scopigno, T. Femtosecond stimulated Raman spectrometer in the 320–520 nm range. *Opt. Express* **2011**, *19*, 1107–1112. [CrossRef] [PubMed]
54. Monacelli, L.; Batignani, G.; Fumero, G.; Ferrante, C.; Mukamel, S.; Scopigno, T. Manipulating impulsive stimulated raman spectroscopy with a chirped probe pulse. *J. Phys. Chem. Lett.* **2017**, *8*, 966–974. [CrossRef] [PubMed]
55. Liebel, M.; Schnedermann, C.; Wende, T.; Kukura, P. Principles and applications of broadband impulsive vibrational spectroscopy. *J. Phys. Chem. A* **2015**, *119*, 9506–9517. [CrossRef] [PubMed]
56. Kuramochi, H.; Takeuchi, S.; Yonezawa, K.; Kamikubo, H.; Kataoka, M.; Tahara, T. Probing the early stages of photoreception in photoactive yellow protein with ultrafast time-domain Raman spectroscopy. *Nat. Chem.* **2017**, *9*, 660. [CrossRef] [PubMed]
57. Batignani, G.; Fumero, G.; Kandada, A.R.S.; Cerullo, G.; Gandini, M.; Ferrante, C.; Petrozza, A.; Scopigno, T. Probing femtosecond lattice displacement upon photo-carrier generation in lead halide perovskite. *Nat. Commun.* **2018**, *9*, 1971. [CrossRef] [PubMed]
58. Zavalin, A.; Cricenti, A.; Generosi, R.; Luce, M.; Morgan, S.; Piston, D. Nano-Raman mapping of porous glass ceramics with a scanning near-field optical microscope in collection mode. *Appl. Phys. Lett.* **2006**, *88*, 133126. [CrossRef]
59. Sonntag, M.D.; Pozzi, E.A.; Jiang, N.; Hersam, M.C.; Van Duyne, R.P. Recent advances in tip-enhanced Raman spectroscopy. *J. Phys. Chem. Lett.* **2014**, *5*, 3125–3130. [CrossRef] [PubMed]
60. Kowalewski, M.; Bennett, K.; Dorfman, K.E.; Mukamel, S. Catching conical intersections in the act: Monitoring transient electronic coherences by attosecond stimulated X-ray Raman signals. *Phys. Rev. Lett.* **2015**, *115*, 193003. [CrossRef] [PubMed]
61. Polli, D.; Altoè, P.; Weingart, O.; Spillane, K.M.; Manzoni, C.; Brida, D.; Tomasello, G.; Orlandi, G.; Kukura, P.; Mathies, R.A.; et al. Conical intersection dynamics of the primary photoisomerization event in vision. *Nature* **2010**, *467*, 440. [CrossRef] [PubMed]
62. Calegari, F.; Ayuso, D.; Trabattoni, A.; Belshaw, L.; De Camillis, S.; Anumula, S.; Frassetto, F.; Poletto, L.; Palacios, A.; Decleva, P.; et al. Ultrafast electron dynamics in phenylalanine initiated by attosecond pulses. *Science* **2014**, *346*, 336–339. [CrossRef] [PubMed]
63. Lara-Astiaso, M.; Galli, M.; Trabattoni, A.; Palacios, A.; Ayuso, D.; Frassetto, F.; Poletto, L.; De Camillis, S.; Greenwood, J.; Decleva, P.; et al. Attosecond Pump–Probe Spectroscopy of Charge Dynamics in Tryptophan. *J. Phys. Chem. Lett.* **2018**, *9*, 4570–4577. [CrossRef] [PubMed]
64. Beaulieu, S.; Comby, A.; Clergerie, A.; Caillat, J.; Descamps, D.; Dudovich, N.; Fabre, B.; Géneaux, R.; Légaré, F.; Petit, S.; et al. Attosecond-resolved photoionization of chiral molecules. *Science* **2017**, *358*, 1288–1294. [CrossRef] [PubMed]
65. Attar, A.R.; Bhattacherjee, A.; Pemmaraju, C.; Schnorr, K.; Closser, K.D.; Prendergast, D.; Leone, S.R. Femtosecond X-ray spectroscopy of an electrocyclic ring-opening reaction. *Science* **2017**, *356*, 54–59. [CrossRef] [PubMed]
66. Marciniak, A.; Despré, V.; Barillot, T.; Rouzée, A.; Galbraith, M.; Klei, J.; Yang, C.H.; Smeenk, C.; Loriot, V.; Reddy, S.N.; et al. XUV excitation followed by ultrafast non-adiabatic relaxation in PAH molecules as a femto-astrochemistry experiment. *Nat. Commun.* **2015**, *6*, 7909. [CrossRef] [PubMed]
67. Nelson, T.R.; Ondarse-Alvarez, D.; Oldani, N.; Rodriguez-Hernandez, B.; Alfonso-Hernandez, L.; Galindo, J.F.; Kleiman, V.D.; Fernandez-Alberti, S.; Roitberg, A.E.; Tretiak, S. Coherent exciton-vibrational dynamics and energy transfer in conjugated organics. *Nat. Commun.* **2018**, *9*, 2316. [CrossRef] [PubMed]
68. Perfetto, E.; Sangalli, D.; Marini, A.; Stefanucci, G. Ultrafast Charge Migration in XUV Photoexcited Phenylalanine: A First-Principles Study Based on Real-Time Nonequilibrium Green's Functions. *J. Phys. Chem. Lett.* **2018**, *9*, 1353–1358. [CrossRef] [PubMed]
69. Ren, X.; Wang, E.; Skitnevskaya, A.D.; Trofimov, A.B.; Gokhberg, K.; Dorn, A. Experimental evidence for ultrafast intermolecular relaxation processes in hydrated biomolecules. *Nat. Phys.* **2018**, *14*, 1062. [CrossRef]

70. Pullen, M.G.; Wolter, B.; Le, A.T.; Baudisch, M.; Hemmer, M.; Senftleben, A.; Schröter, C.D.; Ullrich, J.; Moshammer, R.; Lin, C.D.; et al. Imaging an aligned polyatomic molecule with laser-induced electron diffraction. *Nat. Commun.* **2015**, *6*, 7262. [CrossRef] [PubMed]
71. Erk, B.; Boll, R.; Trippel, S.; Anielski, D.; Foucar, L.; Rudek, B.; Epp, S.W.; Coffee, R.; Carron, S.; Schorb, S.; et al. Imaging charge transfer in iodomethane upon X-ray photoabsorption. *Science* **2014**, *345*, 288–291. [CrossRef] [PubMed]
72. Yang, J.; Zhu, X.; Wolf, T.J.; Li, Z.; Nunes, J.P.F.; Coffee, R.; Cryan, J.P.; Gühr, M.; Hegazy, K.; Heinz, T.F.; et al. Imaging CF3I conical intersection and photodissociation dynamics with ultrafast electron diffraction. *Science* **2018**, *361*, 64–67. [CrossRef] [PubMed]
73. Kraus, P.M.; Zürch, M.; Cushing, S.K.; Neumark, D.M.; Leone, S.R. The ultrafast X-ray spectroscopic revolution in chemical dynamics. *Nature* **2018**, *2*, 82–94. [CrossRef]
74. Kuleff, A.I.; Kryzhevoi, N.V.; Pernpointner, M.; Cederbaum, L.S. Core ionization initiates subfemtosecond charge migration in the valence shell of molecules. *Phys. Rev. Lett.* **2016**, *117*, 093002. [CrossRef] [PubMed]
75. Karydas, A.; Paradellis, T. Measurement of KL and LM resonant Raman scattering cross sections with a proton-induced X-ray beam. *J. Phys. B* **1997**, *30*, 1893. [CrossRef]
76. Leani, J.J.; Sánchez, H.J.; Valentinuzzi, M.; Pérez, C. Determination of the oxidation state by resonant-Raman scattering spectroscopy. *J. Anal. At. Spectrom.* **2011**, *26*, 378–382. [CrossRef]
77. Robledo, J.I.; Leani, J.J.; Karydas, A.G.; Migliori, A.; Pérez, C.A.; Sánchez, H.J. Energy-Dispersive Total-Reflection Resonant Inelastic X-ray Scattering as a Tool for Elemental Speciation in Contaminated Water. *Anal. Chem.* **2018**, *90*, 3886–3891. [CrossRef] [PubMed]
78. Leani, J.J.; Pérez, R.D.; Robledo, J.I.; Sánchez, H. 3D-reconstruction of chemical state distributions in stratified samples by spatially resolved micro-X-ray resonant Raman spectroscopy. *J. Anal. At. Spectrom.* **2017**, *32*, 402–407. [CrossRef]
79. Leani, J.J.; Robledo, J.I.; Sánchez, H.J. Quantitative speciation of manganese oxide mixtures by RIXS/RRS spectroscopy. *X-ray Spectrom.* **2017**, *46*, 507–511. [CrossRef]
80. Robledo, J.I.; Saánchez, H.J.; Leani, J.J.; Pérez, C.A. Exploratory methodology for retrieving oxidation state information from X-ray resonant Raman scattering spectrometry. *Anal. Chem.* **2015**, *87*, 3639–3645. [CrossRef] [PubMed]
81. Leani, J.J.; Sánchez, H.J.; Pérez, C.A. Oxide nanolayers in stratified samples studied by X-ray resonant Raman scattering at grazing incidence. *J. Spectrosc.* **2015**, *2015*, 618279. [CrossRef]
82. Sanchez, H.J.; Leani, J.J.; Pérez, C.; Pèrez, R.D. Arsenic Speciation by X-ray Spectroscopy using Resonant Raman Scattering. *J. Appl. Spectrosc.* **2014**, *80*, 912–916. [CrossRef]
83. Leani, J.J.; Saánchez, H.J.; Pérez, R.D.; Peérez, C. Depth profiling nano-analysis of chemical environments using resonant Raman spectroscopy at grazing incidence conditions. *Anal. Chem.* **2013**, *85*, 7069–7075. [CrossRef] [PubMed]
84. Leani, J.J.; Sánchez, H.J.; Valentinuzzi, M.C.; Pérez, C.; Grenón, M. Qualitative microanalysis of calcium local structure in tooth layers by means of micro-RRS. *J. Microsc.* **2013**, *250*, 111–115. [CrossRef] [PubMed]
85. Leani, J.J.; Sánchez, H.; Valentinuzzi, M.; Pérez, C. Chemical environment determination of iron oxides using RRS spectroscopy. *X-ray Spectrom.* **2011**, *40*, 254–256. [CrossRef]
86. Leani, J.J.; Robledo, J.I.; Sánchez, H.J. Energy dispersive inelastic X-ray scattering (EDIXS) spectroscopy–A review. *Spectrochim. Acta Part B* **2019**, *154*, 10–24. [CrossRef]
87. Chiadroni, E.; Bacci, A.; Bellaveglia, M.; Boscolo, M.; Castellano, M.; Cultrera, L.; Di Pirro, G.; Ferrario, M.; Ficcadenti, L.; Filippetto, D.; et al. The SPARC linear accelerator based terahertz source. *Appl. Phys. Lett.* **2013**, *102*, 094101. [CrossRef]
88. Giorgianni, F.; Anania, M.P.; Bellaveglia, M.; Biagioni, A.; Chiadroni, E.; Cianchi, A.; Daniele, M.; Del Franco, M.; Di Giovenale, D.; Di Pirro, G.; et al. Tailoring of highly intense thz radiation through high brightness electron beams longitudinal manipulation. *Appl. Sci.* **2016**, *6*, 56. [CrossRef]

89. Castellano, M.; Verzilov, V.; Catani, L.; Cianchi, A.; Orlandi, G.; Geitz, M. Measurements of coherent diffraction radiation and its application for bunch length diagnostics in particle accelerators. *Phys. Rev. E* **2001**, *63*, 056501. [CrossRef] [PubMed]
90. Chiadroni, E. Bunch Length Characterization at the TTF VUV-FEL. Ph.D. Thesis, Università degli Studi di Roma "Tor Vergata", Roma, Italy, September 2006.
91. Alesini, D.; Vicario, C.; Bertolucci, S.; Biagini, M.E.; Biscari, C.; Boni, R.; Boscolo, M.; Castellano, M.; Clozza, A.; Di Pirro, G.; et al. *Technical Design Report for the SPARC Advanced Photo-Injector*; Palumbo, L., Rosenzweig, J.B., Eds.; INFN: Pisa, Italy, 2004.
92. Van der Geer, S.; De Loos, M.; Bongerd, D. General Particle Tracer: A 3D code for accelerator and beam line design. In Proceedings of the 5th European Particle Accelerator Conference, Stockholm, Sweden, 10–14 June 1996.
93. Xie, M. Design optimization for an X-ray free electron laser driven by SLAC linac. In Proceedings of the IEEE Particle Accelerator Conference, Dallas, TX, USA, 1–5 May 1995; Volume 1, pp. 183–185.
94. Giorgianni, F.; Chiadroni, E.; Rovere, A.; Cestelli-Guidi, M.; Perucchi, A.; Bellaveglia, M.; Castellano, M.; Di Giovenale, D.; Di Pirro, G.; Ferrario, M.; et al. Strong nonlinear terahertz response induced by Dirac surface states in Bi_2Se_3 topological insulator. *Nat. Commun.* **2016**, *7*, 11421. [CrossRef] [PubMed]
95. Mitrano, M.; Cantaluppi, A.; Nicoletti, D.; Kaiser, S.; Perucchi, A.; Lupi, S.; Di Pietro, P.; Pontiroli, D.; Riccò, M.; Clark, S.R.; et al. Possible light-induced superconductivity in K_3C_{60} at high temperature. *Nature* **2016**, *530*, 461–464. [CrossRef] [PubMed]
96. Chen, H.T.; Kersting, R.; Cho, G.C. Terahertz imaging with nanometer resolution. *Appl. Phys. Lett.* **2003**, *83*, 3009–3011. [CrossRef]